A cascaded Hough transform as an aid in aerial image interpretation

Tinne Tuytelaars, Luc Van Gool, Marc Proesmans, and Theo Moons

VISICS-Lab, ESAT-MI2
Kath. Universiteit Leuven
Kard. Mercierlaan 94, 3001 Leuven, Belgium
Tinne.Tuytelaars,Luc.VanGool,Marc.Proesmans,Theo.Moons@esat.kuleuven.ac.be

Abstract

Cartography and other applications of remote sensing have led to an increased interest in the (semi-)automatic interpretation of structures in aerial images of urban and suburban areas. Building delineation and 3D reconstruction is a good case in point. Although urban and suburban areas are particularly challenging because of their complexity, the degree of regularity in such man-made structures also helps to tackle the problems. The paper presents the iterated application of the Hough transform as a means to exploit such regularities. It shows how such 'Cascaded Hough Transform' yields straight lines, vanishing points, and vanishing lines. It also illustrates how the latter assist in improving the precision of the former. The examples are based on real aerial photographs.

Keywords: Hough transform, aerial image interpretation, remote sensing, vanishing points and lines

1 Introduction

The automatic interpretation of aerial photographs is a challenging task for computer vision. Since the pioneering work of Huertas and Nevatia [6], which focussed on the identification and delineation of man-made structures in aerial images, more and more attention is being paid to the recovery of 3-dimensional (3D) information from stereo pairs and multiple views. Most of the approaches proposed in the literature aim at identifying predefined building models (to various degrees of specification) in the images or in a 3D reconstruction of the scene (see. e.g. [2, 3, 14, 16]). Such a strategy is particularly succesful in industrial areas or sites for official use, where many flat roof and gable roof buildings are encountered. But even in model-based reconstruction, the accuracy of the outcome largely depends on the precision with which the models can be fitted to the data. Therefore is was proposed in [10] (see also [14]) to incorporate as much knowledge about the imaging geometry as possible in the feature extraction stage. In particular, the importance of horizontal and vertical directions in building models provide strong geometric constraints for the image projection of the buildings.

Recently, (semi-) automatic reconstruction of urban and suburban areas has become a topic of increasing importance, because of their usefulness for cartography, cadaster maps and town planning, the detection of changes (e.g. unauthorised building), or the optimal placement of GSM antennas based on 3D models of towns (necessary to predict the propagation of the electro-magnetic waves). Buildings encountered in urban and suburban sites, however, show a much wider variety in their shapes. Many roofs neither are flat nor are composed of simple rectangular shapes. This seriously limits the use of models for their extraction and reconstruction. In [1] it was proposed to model a house roof as a set of planar polygonal patches that mutually adjoin along common boundaries. This allows to model both simple as well as complicated building structures, but this flexibility also increases the need for precision in the extraction of the building primitives from the image data.

In order to arrive at the necessary precision, high resolution imagery has to be used. In our experiments, we used images with a pixel resolution of approximately $8 \times 8\ cm^2$ on the ground. However, buildings and other man-made structures not only show a high degree of geometric regularity at the building level itself, but also at higher levels of spatial hierarchy. For example, at the street level, buildings and other structures tend to be aligned (cf. [16]); and, at still a higher level, streets form block patterns, etc.. These types of regularity can also be exploited in case of non-model-based building extraction, as will be illustrated in this paper. As also will come out, the regularities support the improved detection of the basic line features that are the building blocks for most building detectors.

Concepts like dominant orientations and parallelism have been used many times. Hence, this paper is by far not the first to propose such strategy. Here, a tool is presented that helps to turn these principles into an operational scheme. It is based on the iterative application of a Hough transform. This method will be referred to as the 'Cascaded Hough Transform' or CHT for short. The CHT supports the stratified detection of straight lines, vanishing points and vanishing lines, all of which are powerful cues in aerial image interpretation.

Hough type of schemes have been used before for the detection of structures in aerial images, both as a means to find straight line segments and to detect vanishing points [9, 10]. The novelty of the proposed work is twofold.
First, a cascaded version of the Hough transform – the CHT – is introduced, that finds structures at the different hierarchical levels by iterating one single kind of Hough transform. Previously, Hough transforms were used for line extraction or vanishing point detection, but these steps were not combined into a single scheme. Moreover, the Hough transforms involved were of a different nature. This is discussed in more detail later. Having a single scheme for the extraction of these different features greatly simplifies the interaction between the different levels at which they are found. It is primarily this interaction by which the propounded approach holds good promise.
Secondly, the aerial images to which the method is applied are nadir rather than oblique views. Perspective effects have previously been used almost exclusively for oblique, reconnaissance type of views. Aerial imagery for civil applications has the camera oriented almost vertically, however. Nevertheless, even if the perspective effects are much weaker in such case, the results in the paper show them to be of sufficient import to warrant their explicit detection. Because of the vanishing points and lines 'approaching' infinity, a special parametrisation is proposed for the different Hough spaces involved.

The remainder of the paper is organised as follows. Section 2 describes the CHT (Cascaded Hough Transform) and how it can assist in detecting the regularities at the different levels. This section also discusses some implementation issues. Section 3 shows results on aerial images. They corroborate the need for perspective corrections even in nadir type imagery and also show how the different levels of the CHT each have a role to play in the precise delineation of man-made structures. Section 4 concludes the paper.

2 A cascaded Hough transform

2.1 A new parametrisation of the Hough space

The Hough transform's history stretches a long way back, as P.V.C. Hough ([5]) patented it in 1962. Yet, now it probably has more applications than ever before and it still is the subject of research and a favourite approach to feature extraction for many [7, 8]. Attempts to replace it by alternative schemes such as SLIDE have not been very successful [15].

The Hough transform is a global, robust technique for the detection of predefined shapes in images, esp. straight lines. It is based on the transformation of the edge points to a parameter space. In fact, in its most efficient forms, the Hough transform exploits the symmetry of simple parametric shapes (translational for lines, rotational for circles) in order to reduce the dimensionality of the search [12].

Here, only the extraction of straight lines is considered, although circular structures also sometimes appear in aerial photographs. In the original version of the Hough transform, the lines were given a slope-intercept parametrical representation, i.e. using parameters

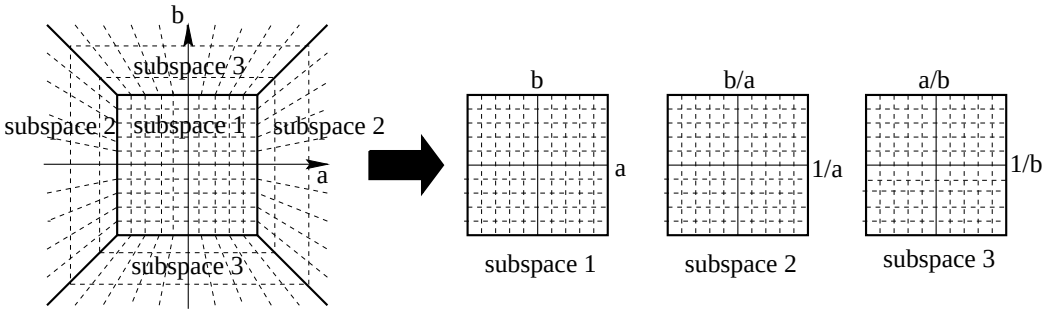

Figure 1: *The original, unbounded space is split into three, bounded subspaces with coordinates* (a, b)*,* $(1/a, b/a)$*, and* $(1/b, a/b)$*, resp.*

(a, b) according to the equation

$$ax + b + y = 0 \ . \tag{1}$$

Using this (a, b)-parametrisation, a pair of edge point coordinates (x, y) is transformed into a line in the (a, b)-parameter space. Similarly, a point with coordinates (a, b) in the Hough parameter space corresponds to a line in the (x, y)-space, i.e. the image. The symmetry in this duality between the two spaces is an important feature of the slope-intercept parametrisation. Indeed, the parameters a and b are to the image space (x, y) what x and y are to the Hough space (a, b). Lines in one space can be detected as points in the other space and, vice versa, for every point there is also a corresponding line.

The problem with the (a, b) space is that it is unbounded. Both a and b can take infinite values, also for lines that are partially visible in the image. Therefore, the polar (r, θ) line parametrisation has been introduced [4]. It is based on the orthogonal distance of the line to the origin (ρ) and the direction of the normal (θ). This parametrisation yields a bounded parameter space. But now a point is transformed to a cosine in parameter space, instead of a line. Hence the symmetry between image space and parameter space is broken.

Here we'll stick to the slope-intersect representation in order to safeguard the duality between the image and the parameter space. Obviously, the unboundedness problem cannot be discarded just like that. In order to restore the boundedness of the parameter space while preserving the symmetric space duality, the (a, b)-space is split into three parts. This is shown in figure 1. The first subspace also has coordinates a and b, but only for $|a| \leq 1$ and $|b| \leq 1$. If $|a| > 1$ and $|b| \leq |a|$, the point (a, b) turns up in the second subspace, with coordinates $1/a$ and b/a. If, finally, $|b| > 1$ and $|a| < |b|$, we use a third subspace with coordinates $1/b$ and a/b. In this way, the unbounded (a, b)-space is split into three subspaces with coordinates restricted to the interval $[-1, 1]$, while a point (x, y) in the original space is still transformed into a line in each of the three subspaces. As can be seen in figure 1, this can also be interpreted as an inhomogeneous discretisation of the unbounded parameter space, with cells growing larger as they get further away from the origin.

The same subdivision is also applied to the (x, y)-image space, yielding three subspaces, with coordinates (x, y), $(1/x, y/x)$ and $(1/y, x/y)$. This stands to reason as (x, y)-space is

in fact also an unbounded space, not restricted to the size of the image itself. Especially in the given context of aerial image interpretation, wanted structures like vanishing points and lines tend to fall far outside the image. With the proposed parametrisation, the points lying at or near infinity are included in a natural way. Moreover, the original image is rescaled, such that the first subspace corresponds to the image itself. In case the image is a square, the image boundaries are given by $x = \pm 1$ and $y = \pm 1$. If the image dimensions are not equal, the first subspace is made to include the smallest square that contains the image. In several applications the image will be a square and then this parametrisation makes explicit positional references such as left from, right from, above or below the field of view, depending on the subspace in which structures are found. This information can have a direct bearing on the behaviour of a mobile robot, for instance, where indoor scenes are often analysed to find straight lines to follow or vanishing points to head for. Cells growing larger when going out of the field of view is in keeping with the fact that points and structures lying further away are normally determined less accurately anyhow and similar shifts in their position have less impact in the image the further away they are.

The subdivision of both spaces doesn't jeopardise the symmetric duality between points and lines. Of course, it complicates matter a little in the sense that a point in one of the 3 image subspaces now yields at least 2 lines with different equations in the 3 parameter subspaces. As an example, suppose a point in the second $(1/x, y/x)$ subspace is considered. It yields the following lines for the parameter subspaces:

$$\begin{aligned} a &+ (1/x)b &+ (y/x) &= 0 \\ (y/x)(1/a) &+ (1/x)(b/a) &+ 1 &= 0 \\ (y/x)(1/b) &+ (a/b) &+ (1/x) &= 0 \end{aligned}$$

Depending on the exact position and slope of the line in (x, y) space, it might be that one of these lines drops out and that the line is only split over two subspaces. In fact, this happens in most of the cases.

Of course, other parametrisations could be considered. A good example is working on a Gaussian sphere [9, 10]. We'll come back to using Gaussian spheres in the section 2.3.

2.2 Iterating the Hough transform

The symmetry of the (modified) slope-intercept parametrisation of section 2.1 makes it possible to repeat the Hough transform on the output of a previous Hough transform. In that manner, one repeatedly switches back and forth between the (x, y) and (a, b)-spaces. This is reminiscent of the use of transform pairs like the forward and backward Fourier. There also one goes to the other domain (i.c. the frequency domain) to perform operations that can be carried out more efficiently there, in order then to go back to the original (spatial) domain and continue part of the operations, possibly before switching again, etc. In contrast to the Fourier transform, the 'forward' and 'backward' Hough transforms as implemented here are identical. Swapping the roles of x, y and a, b resp. is all it takes to

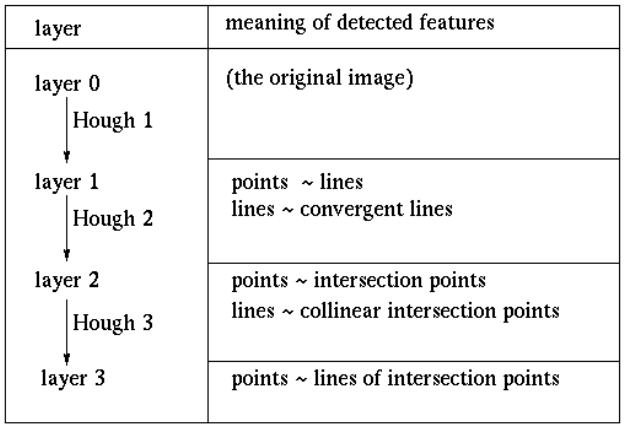

layer	meaning of detected features
layer 0 ↓ Hough 1	(the original image)
layer 1 ↓ Hough 2	points ~ lines lines ~ convergent lines
layer 2 ↓ Hough 3	points ~ intersection points lines ~ collinear intersection points
layer 3	points ~ lines of intersection points

Figure 2: *Flowchart summarising the meaning of the features detected at the different layers of the CHT.*

transcribe the forward into the backward transform. This identity is always advantageous in terms of development time, but especially when dedicated hardware is intended.

In this paper, we propose to apply the Hough transform thrice. Of course, in between different steps the necessary filtering operations will be applied, as outlined in section 2.3.

Figure 2 gives a flowchart summarising the different layers of the CHT. Starting from the image (layer 0), the *first Hough transform* yields a parameter space (layer 1) where peaks correspond to straight lines in the image. Filtering amounts to selecting peaks with a minimal strength.
The *second Hough* is applied to layer 1 with the line related peaks as the only remaining content. This transform yields peaks in a third (x, y) space (layer 2), corresponding to points where several lines intersect. The result is not written into the original (x, y)-space since we want to keep the image intact. Peaks in (a, b) space (layer 1) yielding line intersections in the third (x, y) space (layer 2) is easy to understand as the (a, b)-coordinates of lines going through a single point (x, y) have to be collinear according to eq. (1). This collinearity is picked up by the second Hough. Thus, as the third space (layer 2) is again a (x, y)-space, the peaks in the third space (layer 2) can be interpreted directly as image coordinates of line intersections. Vanishing points are an important case in point. Again, only the peaks (local maxima) are transferred to the next stage.
The *third Hough* detects collinear line intersections (i.e. collinear peaks after the second Hough). If sufficient vanishing points have been found, vanishing lines will stand out at this stage. Again, the (a, b)-peaks in layer 3 have a direct interpretation as line coordinates, but also the (a, b) space is duplicated. The practical importance of this Cascaded Hough Transform not only lies in the additional detection of structures like vanishing points and vanishing lines, but also in the fact that structure found at a higher level can be used to refine the structures found at earlier levels. In section 3 examples are given of how the knowledge of vanishing points help to refine the positions of the straight lines and how

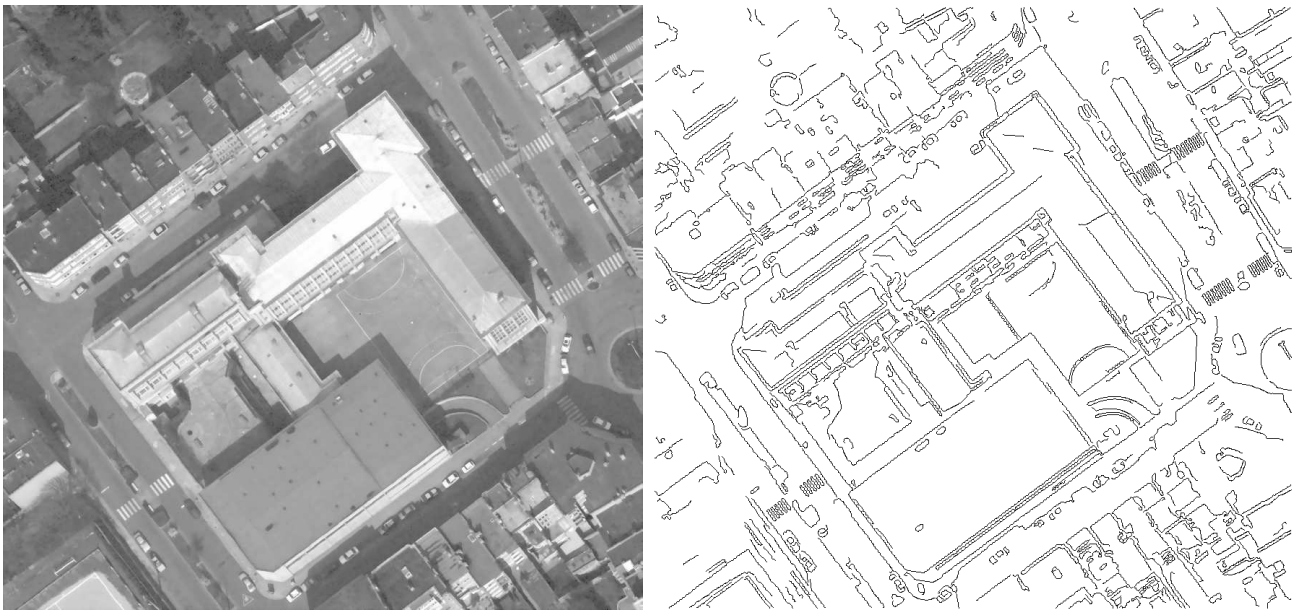

Figure 3: *Aerial image of high resolution with a school building and surrounding streets (left), and the corresponding edges (right).*

vanishing lines in turn increase the precision of the vanishing points.

This section is concluded with an example. Fig. 3 shows an aerial image with two dominant orientations. Fig. 4 shows the different subspaces and layers of the CHT. This figure shows 9 CHT subspaces in total. The first row shows the result of the first Hough transform, the second row that of the second Hough, and the third row the outcome of the third and final Hough transform. The 3 columns correspond to the 3 subspaces, given in the same order as in fig. 1. Peaks in the first row correspond to straight lines in the original image. Some collinear configurations are already salient and correspond to lines intersecting in a single point. These intersections are picked up by the second Hough and hence show up as peaks in the second row. There are two dominant peaks, that correspond to the vanishing points of the two dominant line orientations in fig. 3. Finally, the third row has local maxima at lines that contain at least two intersections. The two dominant peaks of the second row show up as two dominant lines here and their intersection yields the strongest peak of all. This is the horizon line.

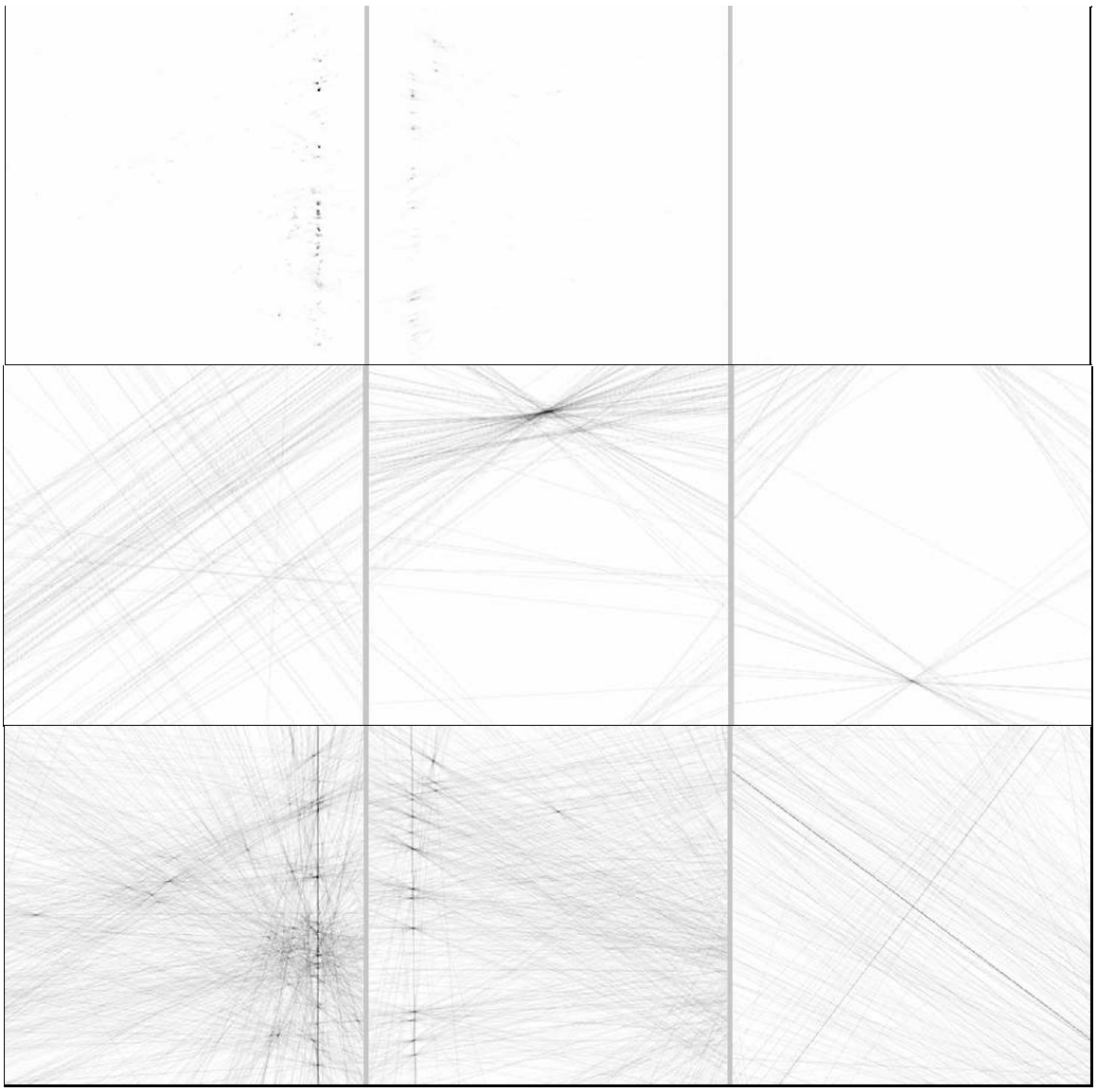

Figure 4: *Nine CHT subspaces for the image of fig. 3. The first, second, and third rows give the results for the first, second, and third Hough, resp. The columns give the first, second, and third subspaces, ordered from left to right according to fig. 1.*

2.3 Implementation of the Cascaded Hough Transform

Before applying a new Hough transform to the result of a previous one, appropriate data filtering is called for. In general, this will include deciding on

1. which data to eliminate from further consideration by subsequent layers,
2. which data to read out as important information emerging at each layer,
3. which data to add to the input of the next Hough Transform.

The third possibility has not been considered yet for this application. As to the data read out at each layer, local maxima are selected. These are also the data passed on to the next Hough transform. First the position of the peaks is determined. These discrete points are the actual inputs to the next layer. In order to avoid closely spaced clusters of peaks, a non-maximum suppression is applied. The logarithm of peak height is used as a weighting factor for the votes it has at the next level. The logarithm expresses the fact that we prefer e.g. four line segments intersecting in a single point than two lines of double length intersecting. The first situation is more non-generic and therefore more conspicious than the first. It should also be noticed that not all edge pixels in the image have been used as input to the first stage, but only those that at least locally already seemed to be part of a straight line. This selection is based on a test on a local line fit. This filters out much of the noise at the very start, and explains the 'clean' subspaces of the first row, as the local line parameters allow us to reduce the extent of the voting pattern (normally a line, here a small blob).

In this example, the image was about 1000×1000 pixels, which is a typical size for the images shown in this paper. The Hough spaces were each about 600×600. Hence, it is fair to say that the CHT requires an appreciable amount of memory.

As an alternative for the parametrisation proposed in this paper, one can use the Gaussian sphere. The Gaussian sphere has been used before, also in the context of aerial image interpretation [9, 10]. In particular, vanishing points have been detected by first fitting straight lines in the image, associating to every line a great circle on the sphere, and then finding places on the sphere where several circles intersect. In the case of Lutton *et al.* [9] a further step would then investigate the relative positions of the intersections on the sphere, in order to find orthogonal directions.
In fact, on the Gaussian sphere a CHT can be defined as follows. It is based on associating great circles (instead of lines) to points and v.v. A first step is to project the points of an image onto a half-sphere through the center of projection. Every point can be interpreted as representing a viewing direction. The Hough transform then goes to a second sphere, where the great circle is drawn that has the original point as its normal direction. If points lie on a straight line in the image, these great circles intersect in a point, which is the normal to the great circle that is formed by projecting the line onto the sphere. Also this modified scheme can be used iteratively. The first Hough yields lines, the second one yields vanishing points. It again is based on taking the peaks on the second sphere, drawing for each a great circle on a third sphere normal to the direction of the point. There intersecting

circles indicate vanishing points. A similar transform to a fourth sphere yields peaks that give normals to the planes of vanishing lines. Again, the transform is identical throughout all the steps.

Working with the Gaussian sphere yields a natural representations of 3D orientations. If the projection from the image plane onto the sphere can proceed with the correct coordinates (focal length, principal point, pixel sizes), the points on the sphere will indeed be faithful representations of the true viewing directions and angles between them will also be correct. If these parameters are unknown, the forementioned construction based on the great circles and normal directions is still possible, but orthogonality of directions on the sphere no longer reflects orthogonality in real space. With the Gaussian spere there are some additional problems of how to tesselate it into voting bins, however [13, 9].

3 Application of the CHT to aerial images

The experiments in this section show that each of the 3 levels of the CHT – finding line structures, finding vanishing points, and finding vanishing lines – contribute to a better delineation of buildings. The Hough transform is a popular tool for line detection in aerial image interpretation, hence we mainly focus on the two additional steps.

3.1 Exploiting vanishing points

Finding straight lines with high precision is one of the major goals behind this work. In this section, examples are shown on how the CHT can improve on results obtained from traditional single-step Hough transforms or from assumptions about edge parallelism.

Consider again fig. 3a. Fig. 3b shows the edges found with a Canny type edge detector. There are two dominant edge orientations in this image. Especially for the orientation going from top-left to bottom-right, there is a perspective effect that cannot be discarded. First, it is interesting to focus on the pedestrian walkway with this orientation, that is visible at the left side of the image. Fig. 5a shows the line that is obtained from a single application of the Hough transform. Although it is positioned rather well, this line does not follow the walkway precisely. Part of the problem are the cars and their shadows that have pulled the edge to the right.

One can expect a better result, by pooling information on the corresponding, dominant orientation. Therefore, the average orientation of the different Hough-based lines belonging to this group was calculated. Only sufficiently long straight edge segments were used, as indicated in fig. 7a. They were found as segments along the lines corresponding to peaks in the first Hough space where contrast over the lines was sufficiently high. This threshold was set quite conservatively. Fig. 5b shows a second estimate for the walkway edge. It has the average orientation and runs through the center of gravity of the walkway segments in fig. 7a. This line follows the walkway edge more closely. A deviation from the real edge is still visible, however. The edge should be rotated slightly clockwise. This is a deviation that is in agreement with what we would expect from the perspective distortion

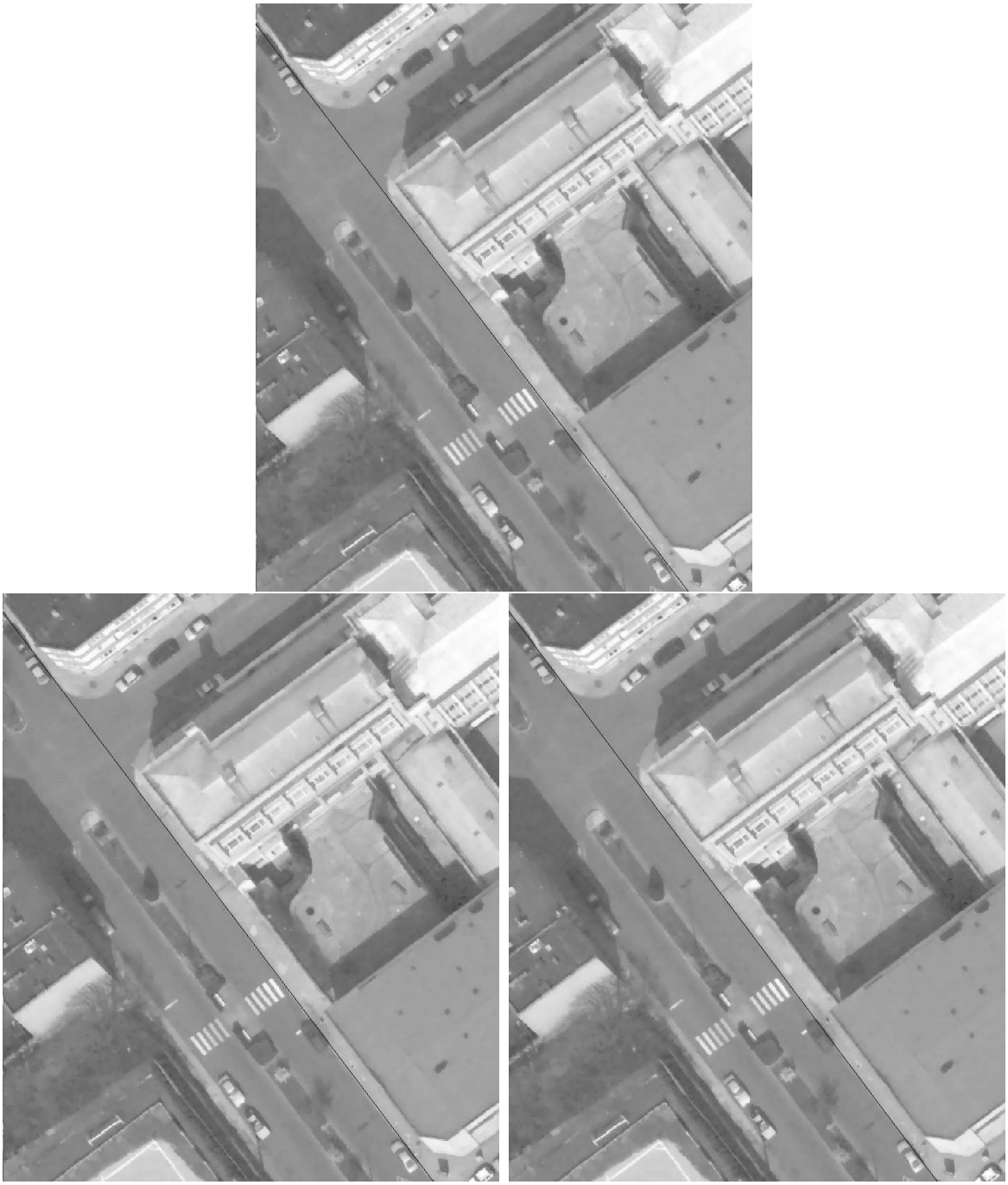

Figure 5: *The line detected by the first Hough-transform (top) clearly is not very accurate. One can improve the orientation of this line by giving it the average orientation of that direction (bottom left). However, a better result is obtained if the line is adapted using the vanishing point of that direction (bottom right).*

Figure 6: *A detail of fig. 3 with the three lines fitted to the walkway: the Hough line at the right, the average line in the middle and the line through the vanishing point at the left.*

Figure 7: *a/ Line segments belonging to the same direction as the walkway (top) b/ idem, after adapting the orientation of the lines such that they pass through the vanishing point (bottom).*

Figure 8: *Aerial image of high resolution with two intersecting streets.*

in the image. Finally, fig. 5c shows another line, through the same center of gravity and the vanishing point corresponding to this dominant orientation. The vanishing point was found after the second step of the CHT. As the system keeps track of the lines that contribute to the different vanishing points, they are easy to match. As can be seen in the figure, the line now follows the walkway edge more closely.

The relative quality of the three edge estimations is better illustrated on a detail near the bottom of the image, because there the differences show up most clearly. Fig. 6 shows that part of the walkway. The three lines are shown together with, from top to bottom, the line found on the basis of a single Hough, based on the averaged orientation, and based on the vanishing point. Only the latter line remains within a 1-pixel distance from the visual edge throughout the image. A similar correction can be applied to the other lines of the same direction. When looking again for support along these lines, we now find longer edge segments (fig. 7b).

As a second example, consider fig. 8, that shows the image of two streets and the corresponding edges found with the Canny edge detector. Based on the CHT, the vanishing points of the main orientations can be determined. Since the facades of the houses are slightly visible, several nearly parallel edges are found. As a result, the line that is detected by the application of the first Hough transform, shown in fig. 9a, is quite off at most roof edges, especially at the lower right half of the image.

Again, taking the center of gravity of the different line segments found and drawing the line through that point and the vanishing point to which the line contributes yields a new line, shown in fig. 9b. This line is much better aligned with the roof edges.

These results show that the detection of vanishing points is not only useful to find

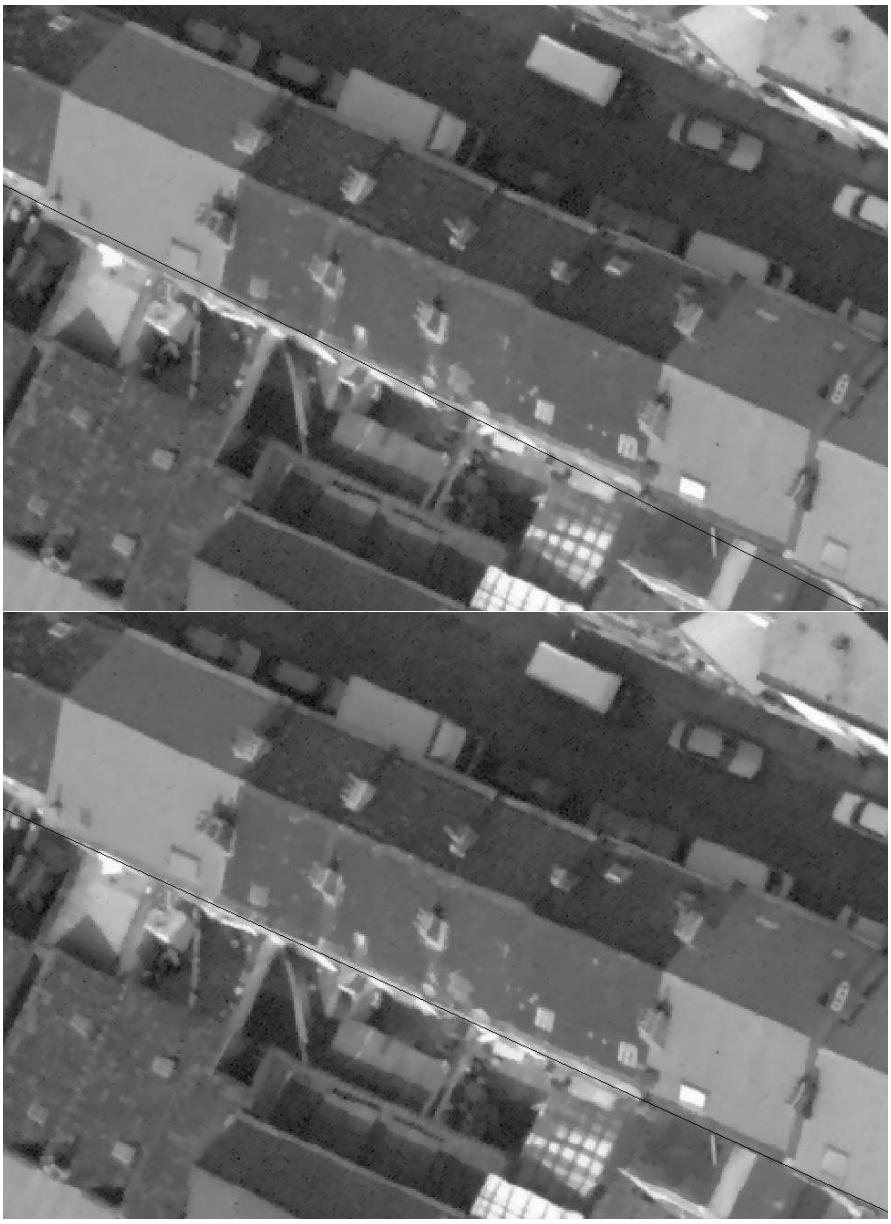

Figure 9: *Lines fitted to the roof edges, using the original Hough line (top) and using the vanishing point (bottom).*

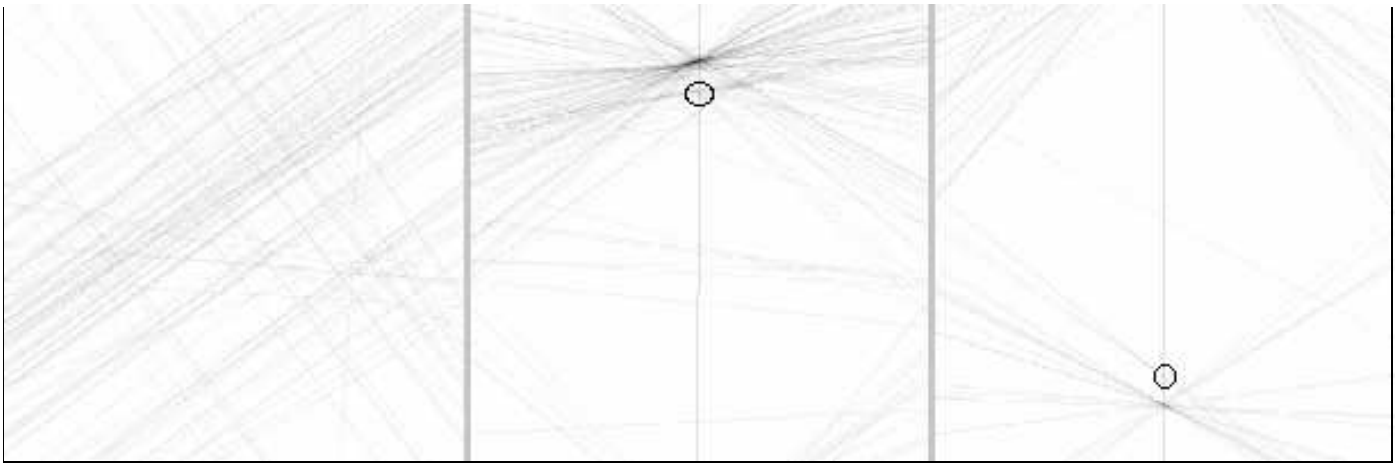

Figure 10: *Second layer of the CHT for the image of fig. 3 with the vanishing line added. Through the use of the vanishing line two new peaks can be detected.*

additional lines or to get insight into the relations between lines; they also help to improve on the precision of the very lines that contributed to their detection. This is the kind of feedback from higher to lower hierarchical levels hinted at in the introduction.

3.2 Exploiting vanishing lines

Finding vanishing lines – such as the horizon – can be useful in its own right. Here the third level of the Hough transform is used in a similar way as the vanishing points were. Their position can be used to increase the precision of vanishing points – the structures found one level below and which in turn give better line fits. Moreover, vanishing points lying on the vanishing line might be important for the scene structure too, although they possibly did not stand out clearly after the second Hough transform. Knowledge of the vanishing line allows their extraction.

As an example, another part of fig. 3a can be used. The top right corner region contains a number of edges that are almost, but not quite parallel with the orientation we have considered before. The corresponding vanishing point is far less outspoken than the earlier one, and hence can hardly be detected. However, several vanishing points are collinear, and yield a peak for a vanishing line (the horizon) after the third Hough transform. One level lower, after the second Hough, the corresponding line can be used to determine the position of vanishing points with lower and smeared peaks with far higher precision. Fig.10 shows again the second layer of the CHT, but this time the line corresponding to the horizon is added. By looking for peaks along this line, two more peaks clearly come out, that had gone unnoticed previously. They correspond to the two orthogonal directions of the houses in the top right corner of the figure.

Once these vanishing points have been detected, they can again be used to improve the accuracy of the corresponding lines. An example is given in fig. 11. The orientation of the original Hough line is not really accurate. But this can be improved based on the position

Figure 11: *Different lines fitted to the roofs: the original Hough line (left) and the line through the vanishing point (right).*

of the corresponding vanishing point.

4 Conclusions and future work

For cases with completely calibrated cameras we also plan to implement the CHT based on the normal/great circle dualism on a Gaussian sphere. In that case the orthogonality of the normal and the circle has a similar interpretation in 3D space and this would better warrant the additional efforts needed for the approximately homogeneous sampling of the Gaussian sphere.

Of course, all kinds of refinements are possible and the results as shown can be improved upon further in order to arrive at a fully automated selection of relevant structures at the different CHT levels. For instance, once dominant peaks have been found, the image features that contributed can be removed (but not the peaks themselves which can still reinforce the weaker peaks at the next levels!), in order to ease the detection of less outspoken peaks.

References

[1] F. Bignone, O. Henricsson, P. Fua and M. Stricker, Automatic extraction of generic house roofs from high resolution aerial imagery, in : B. Buxton and R. Cipolla (eds.), *Computer Vision – ECCV'96*, LNCS **1064**, Springer-Verlag, Berlin / Heidelberg / New York / Tokyo, 1996, pp. 85–96.

[2] A. Brunn, E. Gülch, F. Lang and W. Förstner, A Multi-Layer Strategy for 3D Building Acquisition, in : *Mapping Buildings, Roads and other Man-Made Structures from Images, Proceedings IAPR TC-7 Workshop, Graz, 1996*, Oldenbourg, Wien / München, 1997, pp. 11–37.

[3] R.T. Collins, A.R. Hanson, M.R. Riseman and H. Schultz, Automatic extraction of buildings and terrain from aerial images, in : *Automatic extraction of man-made objects from aerial and space images*, Birkhäuser-Verlag, Basel, 1995, pp. 169–178.

[4] R.O. Duda, P.E. Hart, *Use of the Hough transform to detect lines and curves in pictures*, Commun. ACM 15, pp11-15, 1972.

[5] P.V.C. Hough, *Method and Means for Recognising Complex Patterns*, U.S. Pattern No. 3069654, 1962.

[6] A. Huertas and R. Nevatia, Detecting buildings in aerial images, *Computer Vision, Graphics and Image Processing (CVGIP)*, Vol. **41** (1988), pp. 131–152.

[7] J. Illingworth, J. Kittler, *A survey of the Hough transform*, CVGIP44, pp87-116, 1988.

[8] V.F. Leavers, *Which Hough transform ?*, CVGIP Vol.58, no.2, pp250-264, 1993.

[9] E. Lutton, H. Maître, J. Lopez-Krahe, *Contribution to the Determination of Vanishing Points Using Hough Transform*, PAMI, Vol.16, no.4, 1994.

[10] J. McGlone and J. Shufelt, *Projective and object space geometry for monocular building extraction*, Proc. Conf. Computer Vision and Pattern Recognition, Seattle, pp. 54-61, 1994

[11] G. McLean and D. Kotturi, *Vanishing point detection by line clustering*, IEEE Trans. Pattern Anal. and Machine Intell., Vol. 17, No. 11, pp. 1090-1095, 1995

[12] D. Pintsov, *Invariant pattern recognition, symmetry, and the Radon transform*, J. of the Optical Soc. of America A, Vol. 6, No. 10, pp. 1544-1554, oct. 1989

[13] L. Quan and R. Mohr, *Determining perspective structures using hierarchical Hough transform*, Pattern Recognition Letters, Vol. 9, pp. 279-286, 1989

[14] M. Roux and D. Mc Keown, Feature matching for building extraction from multiple views, *Proceedings of the ARPA Image Understanding Workshop (IUW'94)*, Monterey, CA, 1994, pp. 331–349.

[15] J. Sheinvald and N. Kiryati, *On the magic of SLIDE*, Machine Vision and Applications, No. 9, pp. 251-261, 1997.

[16] U. Stilla , E. Michaelsen and K. Luetjen, Automatic extraction of buildings from aerial images, in : F. Leberl, R. Kalliany and M. Gruber (eds.), *Methods for extracting and mapping buildings, roads and other man-made structures from images*, Oldenburg, Wien / München, 1996.